Surface & Coatings Technology 205 (2011) 4528–4531

Contents lists available at ScienceDirect

Surface & Coatings Technology

journal homepage: www.elsevier.com/locate/surfcoat

Nanoscale friction of partially oxidized silicon nitride thin films

J. Filla [a], C. Aguzzoli [a,b], V. Sonda [a], M.C.M. Farias [a], G.V. Soares [b], I.J.R. Baumvol [a,b], C.A. Figueroa [a,*]

[a] Centro de Ciências Exatas e Tecnologia, Universidade de Caxias do Sul, Caxias do Sul, 95070-560, Brazil
[b] Instituto de Física, Universidade Federal do Rio Grande do Sul, Porto Alegre, 91509-970, Brazil

ARTICLE INFO

Article history:
Received 2 February 2011
Accepted in revised form 25 March 2011
Available online 31 March 2011

Keywords:
Silicon nitride
Silicon oxide
Nanoscale friction
Ionic potential

ABSTRACT

The nanoscale friction of partially oxidized silicon nitride thin films deposited by reactive magnetron sputtering was investigated. Post deposition thermal annealing in O_2, trying to simulate the oxidation by atmospheric oxygen in working conditions, formed a partially oxidized layer at the surface with maximum thickness around 10 nm. Unidirectional sliding tests showed a decrease of the low-load friction coefficients of the sliding pair for the samples annealed in oxygen as compared to the non-annealed ones. The results are discussed on the lights of our extension of the crystal chemistry model, which establishes a relationship between ionic potential and friction coefficient.

1. Introduction

There is currently a trend to avoid the use of liquid lubricants in cutting and machining of metallic and ceramic parts, due to environmental issues and production costs [1]. However, friction in dry conditions increases the temperature of both contacting surfaces up to more than 1100 °C, leading to oxidation and to changes in the mechanical properties of the original material, as well as to modifications in the tribological behavior of the system [2,3]. In order to control these phenomena, the tribology of the system must be understood in detail. Recently, several physicochemical concepts and models have been used to explain the relationships between the nature or products of tribochemical reactions and friction [4–8]. For example, deuterium chemisorbed on diamond or silicon surfaces leads to nanoscale friction coefficients lower than hydrogen chemisorbed on the same surfaces [5]. This was attributed to the lower natural frequency of the carbon (silicon)–deuterium bond as compared to the carbon(silicon)–hydrogen bond, which implies a reduction in the rate at which the kinetic energy of the tip is dissipated. Other advances were reached based on a model, to be discussed below, that connects the ionic potential (φ) and the average friction coefficient of various oxides [7,8].

Silicon nitride (Si_3N_4) is a ceramic material with a relatively high hardness, thermodynamic stability, and oxidation resistance at high temperatures [9,10]. Most of the cutting-edge coating materials used in dry machining operations which have been developed by plasma deposition technologies, contain Si_3N_4 as a main component in several nanocomposite systems [11,12]. Although the hardness of Si_3N_4 can achieve a new maximum (~22 GPa) at 1000 °C due to a well established phase transition (amorphous to alpha) [13], the role of Si_3N_4 in maintaining the hardness and wear resistance of composites at high temperatures is still not fully understood.

The aim of the present study is to investigate both the nanoscale friction and mechanical properties of partially oxidized Si_3N_4 thin films, in an attempt to contribute to clarifying the low friction and hardness stability at high temperatures of this material.

2. Materials and experimental procedure

Si_3N_4 films were deposited on Si(001) substrates by radio frequency (RF) reactive magnetron sputtering. Prior to deposition, substrates were cleaned in ultrasonic acetone bath, followed by a second cleaning step in 10% hydrofluoridric acid solution and immediately loaded in the sputtering vacuum chamber, which was pumped down to a base pressure of 5×10^{-5} Pa. A 2 inch diameter, high purity (>99.99%) silicon target was used, located 60 mm away from the substrate, and Si_3N_4 film depositions were performed using a mixture of argon and nitrogen gasses, with a constant partial pressure of 3×10^{-1} Pa in both cases. Such partial pressures guarantee a Si:N stoichiometry of 3:4, for sample temperatures during deposition (hereafter called DT) higher than 100 °C, as determined by Rutherford backscattering spectroscopy (RBS). An input RF power density of 7.4 $W\cdot cm^{-2}$ was employed with a reflected power density lower than 0.05 $W\cdot cm^{-2}$. DT was varied from room temperature (23 °C) to 500 °C. The deposition time was fixed in 300 s in order to achieve a final thickness of 500 nm in all samples. No delamination of the films was observed.

In order to simulate high temperature oxidation of the as-deposited Si_3N_4 coatings in machining or cutting conditions, samples were loaded in a static pressure, resistively heated quartz furnace, which was pumped down to 2×10^{-5} Pa, before being pressurized with oxygen enriched to 97% in the isotope of mass 18. Oxidation

* Corresponding author.
E-mail address: cafiguer@ucs.br (C.A. Figueroa).

0257-8972/$ – see front matter © 2011 Elsevier B.V. All rights reserved.
doi:10.1016/j.surfcoat.2011.03.111

annealing (hereafter called OA) was performed here in 10^4 Pa of $^{18}O_2$ for 4 h at two different temperatures, namely 500 °C or 1000 °C. The use of the ^{18}O rare isotope allows us to distinguish it from the oxygen previously incorporated in the films due to contamination during deposition or to atmospheric air exposure.

The elementary compositions of the films were quantitatively determined by RBS with a sensitivity of 10^{14} atoms × cm^{-2} (about 1/10 of a monolayer) and 10% accuracy [14]. The hardness and friction measurements were accessed by nanoindentation and nanoscale sliding wear tests, respectively, using a NanoTest-600 equipment manufactured by Micro Materials Ltd, equipped with a three-sided pyramidal diamond tip (Berkovich indenter). The unloading portion of load-depth curves was analyzed, allowing estimating values for film hardness [15]. Nanoindentation tests were performed at a load rate of 0.1 mN·s^{-1} and a maximum indentation depth of 50 nm. The substrate effect on hardness measurements appears when the indentation depth reaches between 10% and 20% of the total thickness. In order to avoid the substrate effect, we chose the lower limit (10%) to perform our measurements. Normal loads of 5, 10, and 20 mN were applied to the Berkovich indenter (used as the counter-face) and the samples were then displaced once at a rate of 1 μm·s^{-1} to a total distance of 300 μm. The tangential force was measured by a load cell and its average steady-state value was related to the friction force of the layer formed at the surface of the Si_3N_4 films before and after OA. The ^{18}O profiles were determined by narrow nuclear resonant reaction profiling [16] (NRP) using the narrow resonances (Γ = 100 eV) in the cross section curves of the $^{18}O(p,\alpha)^{15}N$ nuclear reactions at 151 keV. Simulations of the nuclear reaction excitation curves were carried out using the FLATUS code [17]. The wear tracks were analyzed using a Shimadzu SSX-550 scanning electron microscope (SEM) in secondary electron mode. The characterization of the Si_3N_4 films, before and after annealing in oxygen was performed by the authors and published elsewhere [13].

3. Results and discussion

Fig. 1 shows the oxygen content (%) as a function of depth in the Si_3N_4 thin films deposited at different DT and submitted to OA at 500 °C or 1000 °C, as obtained from the NRP measurements. Here, 100% corresponds to the concentration of ^{18}O in a film made of $Si^{18}O_2$, used as a standard. One can see that very thin partially oxidized layers, only a few nanometers thick were obtained. The oxygen profiles in Si_3N_4 are erfc-like, indicating a diffusion-limited process. In addition, for 4 h of OA the thickness of the oxidized layers was similar to those obtained in a previous work [13] for OA during 1 h.

Fig. 2 shows the hardness versus DT of Si_3N_4 thin films before and after OA, indicating that the hardness increased slightly with DT, reaching maxima of 20–22 GPa. The hardness, on the other hand, did not change significantly after OA. Such mechanical stability in a wide range of temperatures allows the use of Si_3N_4 films in cutting and machining applications where high temperatures are developed.

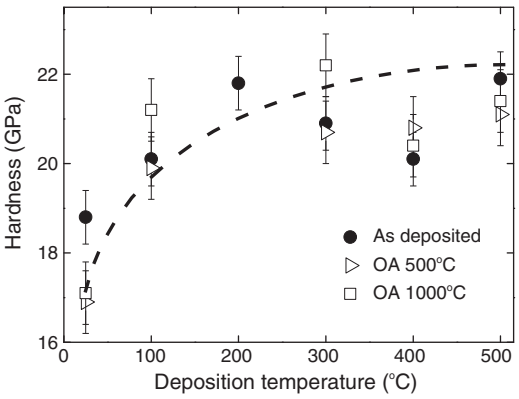

Fig. 2. Hardness profiles versus substrate temperature during deposition of Si_3N_4 thin films before and after oxygen annealing.

Fig. 3 shows the friction coefficients as a function of the sliding distance at different normal loads for Si_3N_4 thin films, DT = 500 °C, before and after OA at 500 °C or 1000 °C, respectively. The average steady-state friction coefficient values (AFC) are also shown for each

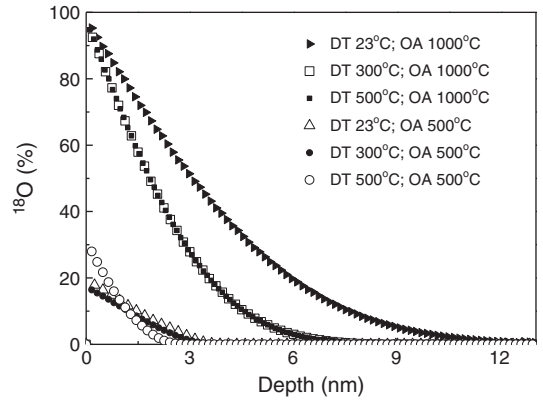

Fig. 1. Oxygen content (%), obtained from the narrow resonant nuclear profiling, as a function of depth in Si_3N_4 thin films deposited at different substrate temperatures and annealed in oxygen at 500 °C or 1000 °C.

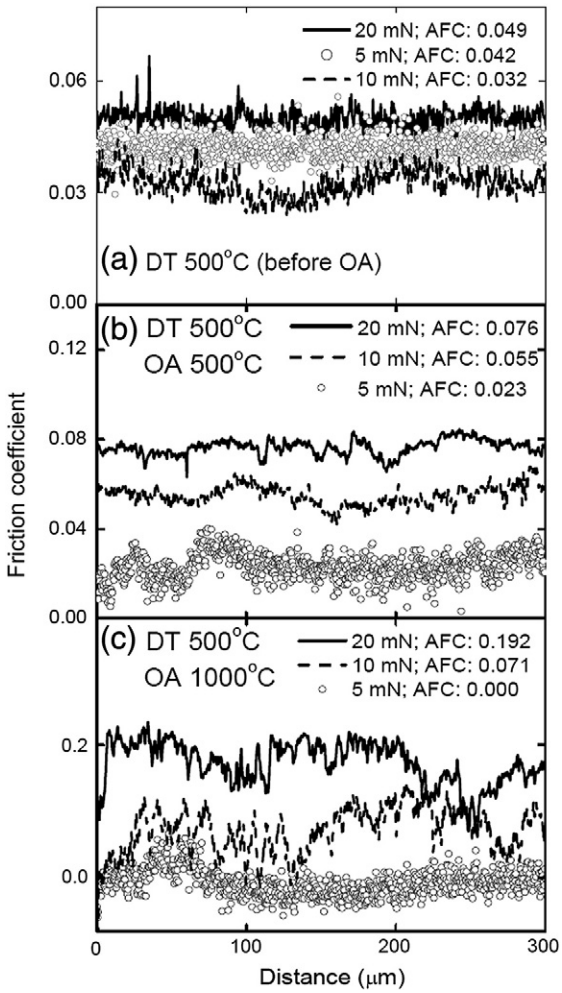

Fig. 3. a–c. Friction coefficient versus sliding distance at different normal loads for Si_3N_4 thin films deposited at 500 °C, before and after annealing in oxygen at 500 °C or 1000 °C, respectively. The average friction coefficients for each curve are also shown.

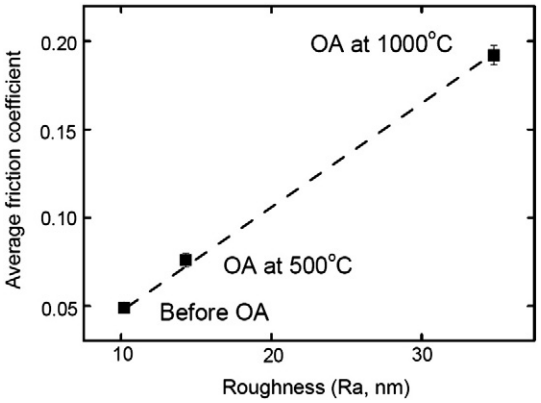

Fig. 4. Average friction coefficients versus surface roughness for Si_3N_4 thin films deposited at 500 °C, before and after annealing in oxygen at 500 °C or 1000 °C.

condition. The as-deposited samples displayed friction coefficients with low dispersion among curves, such that the average steady-state friction coefficient values did not change more than 0.01 for different normal loads (see Fig. 3a). The friction coefficients determined in the present work for the films before OA (0.04 ± 0.01) can be considered load independent. For the samples after OA, the friction coefficients vary substantially with load. Repeated measurements in the same sliding conditions confirmed the above reported results. Furthermore, a similar behavior was observed here in Si_3N_4 thin films deposited at lower substrate temperatures before and after OA. The friction coefficient depends on several parameters in the macro, micro, and nano-scales as, for instance, surface roughness. The surface roughness of the samples was measured simultaneously with the friction coefficient measurements. Fig. 4 shows that surface roughness increases with the increase of the OA temperature. Consequently, the increase in friction coefficient after OA can be attributed to the increase of surface roughness. Furthermore, the number of asperity contacts and interlocking asperities of rubbing surfaces also increases with the increase of the normal load to 10 mN and 20 mN, which is another cause for the increase of the friction coefficient. Finally, higher normal loads can lead to plastic deformation of the soft substrate material, the Si_3N_4 film and the oxide layer. This contact mechanism may result in a higher friction coefficient.

Fig. 5 shows two relevant facts that may contribute to explain such experimental results. Considering Si_3N_4 films deposited at DT = 500 °C and OA at 1000 °C, followed by runs with normal loads of 5, 10, and 20 mN, one notices that the indenter tip penetrated the films up to depths of 110, 190, and 260 nm, respectively. In those sliding conditions, the films did not suffer spalling and, consequently, the measured friction coefficients correspond to those of well adhered Si_3N_4 films on silicon (100) obtained at different DT before OA (Fig. 3a) and to those partially oxidized layers (Fig. 1) formed after OA (Fig. 3b and c). Fig. 5a shows a drawing of the Berkovich indenter toward the inside of the film at a peak load of 20 mN. Trigonometric calculations give a maximum length of the projected contact side of 900 nm at 260 nm indentation depths, in agreement with the SEM image where the width of the wear track is roughly 1000 nm wide (Fig. 5b). Considering the area function of an ideal Berkovich tip, the proportion of oxynitride in contact to the indenter is 17.4%, 10.3%, and 7.5% for normal loads of 5 mN, 10 mN, and 20 mN, respectively. Thus, a lower penetration depth yields a higher oxide proportion in contact with the indenter.

The results shown above can be discussed on the lights of crystal chemistry models. There is an established relationship between ionic potentials ($\varphi = Z/r$) and average friction coefficient of various oxides [7,8]. Here, Z stands for the cationic charges and r for the cation radii. Oxides with higher ionic potentials (cations with higher charge and/or smaller radius) show screened cations by surrounding anions and hence their friction coefficients are lower. From a strictly electrostatic point of view, compounds that have higher Z/r, i. e. a higher cation screening, show a higher near surface electronic density allowing better electrostatic repulsion of the tribologic counterpart. These compounds are considered as lubricious oxides in the tribology literature. Here, we extend the crystal chemistry approach by applying the model to oxide and nitride systems and also by adopting the charge density, located at cationic centers, instead of the so far used valence number for Z. According to data in the literature [18–20], Z/r is 2.03 for Si_3N_4 and 3.59 for SiO_2 and therefore the low-load friction coefficient of partially oxidized Si_3N_4 films should be lower than that of non-oxidized ones, in good agreement with the present experimental results. The ionic potentials calculated here are lower than previous ones [7], owing to the absolute values of the used density charges being lower than the valence numbers. Besides chemical interactions, surface roughness can also be responsible for the friction behavior (see Fig. 4). However, the influence of increasing surface roughness with oxidation annealing in friction coefficient is negligible at the lowest normal load (5 mN), due to the reduced contact area as the result of the small number of asperity contacts. After OA, the formation of the oxynitride layer SiO_xN_y with low shear strength on the top of the Si_3N_4 thin film may result in a low friction

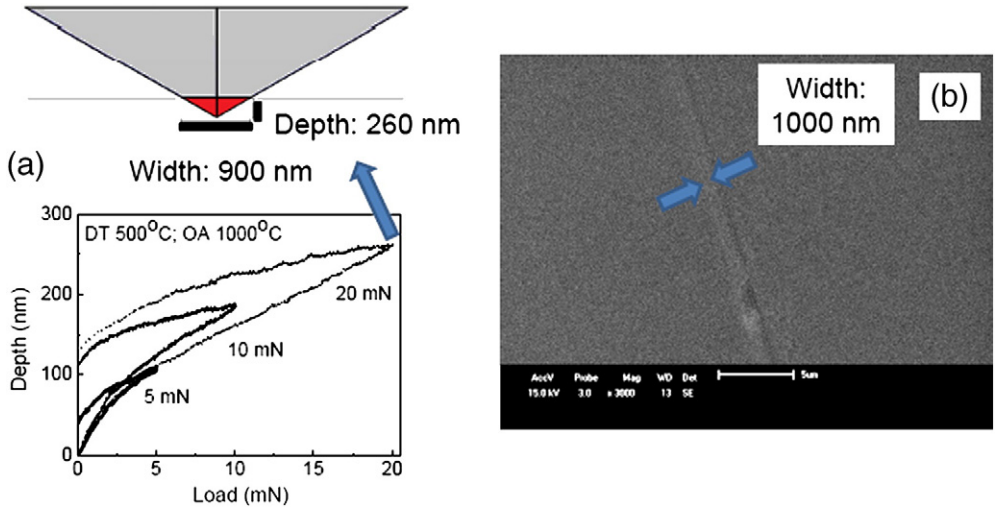

Fig. 5. a and b. Scheme of the indenter tip penetrating the oxygen annealed Si_3N_4 thin film and indentation curves at normal loads of 5, 10, and 20 mN (a). SEM image of a wear track on a well adhered Si_3N_4 thin film deposited at 500 °C and annealed in oxygen at 1000 °C (b).

coefficient. Thus, the friction behavior at 5 mN for both the untreated and OA treated samples can be explained by the crystal chemical model.

4. Conclusions

In summary, Si_3N_4 thin films were deposited on Si at different substrate temperatures. Nanoindentation and low-load sliding experiments were performed in order to study the hardness and friction behavior before and after oxygen annealing in O_2, trying to simulate high temperature oxidation by atmospheric oxygen in working conditions. Si_3N_4 has a high oxidation resistance, such that a very thin oxide layer, approximately 10 nm thick, is obtained at 1000 °C and 4 h of OA. The presence of such partially oxidized layer decreases the friction coefficient at low loads even when a higher surface roughness is observed. The crystal chemistry approach was expanded here to calculate the ionic potentials (Z/r ratio) in oxides and nitrides (SiO_2 and Si_3N_4), adopting the charge density, located at cationic centers, instead of the so far used valence number for Z. The higher ionic potential of SiO_2 as compared to that of Si_3N_4 indicated that, according to the present approach, the friction coefficient of partially oxidized Si_3N_4 films should decrease after oxidation, in agreement with the experimental results shown above. In dry cutting or machining conditions, Si_3N_4 films retain their hardness. Furthermore, at the high surface temperatures developed during dry machining, the atmospheric oxygen renews the oxidation of the surface of the Si_3N_4 coating, decreasing the friction coefficient of the tribosystem and, finally, preventing further mechanical damage. Finally, we recall here the very low values for the friction coefficient at a normal load of 5 mN, which were obtained after thermal annealing in O_2.

Acknowledgments

This work was partially sponsored by CNPq: projects # 573628/2008-4 (National Institute of Surface Engineering) and # 550316/2007-8 (Young Researcher). IJRB and CAF are CNPq fellows.

References

[1] J. Gerth, M. Larsson, U. Wiklund, F. Riddar, S. Hogmark, Wear 266 (2009) 444.
[2] G.S. Fox-Rabinovich, K. Yamamoto, B.D. Beake, A.I. Kovalev, M.H. Aguirre, S.C. Veldhuis, G.K. Dosbaeva, D.L. Wainstein, A. Biksa, A. Rashkovskiy, Surf. Coat. Technol. 204 (2010) 3425.
[3] Y.C. Chim, X.Z. Ding, X.T. Zeng, S. Zhang, Thin Solid Films 517 (2009) 4845.
[4] S.H. Li, V. Palekar, Tribology 3 (2009) 132.
[5] R.J. Cannara, M.J. Brukman, K. Cimatu, A.V. Sumant, S. Baldelli, R.W. Carpick, Science 318 (2007) 780.
[6] B. Bhushan, J.N. Israelachvili, U. Landman, Nature 374 (1995) 607.
[7] A. Erdemir, Surf. Coat. Technol. 200 (2005) 1792.
[8] A. Erdemir, S. Li, Y. Jin, Int. J. Mol. Sci 6 (2005) 203.
[9] A. Ziegler, J.C. Idrobo, M.K. Cinibulk, C. Kisielowski, N.D. Browning, R.O. Ritchie, Science 306 (2004) 768.
[10] Y. Toivola, J. Thurn, R.F. Cook, J. Appl. Phys. 94 (2003) 6915.
[11] S. Veprek, M.G.J. Veprek-Heijman, R. Zhang, J. Phys. Chem. Sol. 68 (2007) 1161.
[12] Q.F. Fang, Q. Liu, S.Z. Li, Z.S. Li, P. Karvankova, M. Jilek, S. Veprek, Mater. Sci. Eng. A 442 (2006) 328.
[13] C. Aguzzoli, C. Marin, C.A. Figueroa, G.V. Soares, I.J.R. Baumvol, J. Appl. Phys. 107 (2010) 073521.
[14] L.C. Feldman, J.W. Mayer, S.T. Picraux, Materials Analysis by Ion Channeling, Academic Press, New York, 1982.
[15] W.C. Oliver, G.M. Pharr, J. Mater. Res. 7 (1992) 1564.
[16] I.J.R. Baumvol, Surf. Sci. Rep. 36 (1999) 1.
[17] R.P. Pezzi, P.L. Grande, M. Copel, Surf. Sci. 601 (2007) 5559.
[18] Z. Liu, S. Sugata, K. Yuge, M. Nagasono, K. Tanaka, J. Kawai, Phys. Rev. B 69 (2004) 035106.
[19] G.L. Zhao, M.E. Bachlechner, Phys. Rev. B 58 (1998) 1887.
[20] R.E. Smallman, R.J. Bishop, Modern Physical Metallurgy & Materials Engineering, 6th ed., Butterworth-Heinemann, Oxford, 1999.